EDGE ARTICLE

Enantioselective aromatic Claisen rearrangement of allyl 2-naphthyl ethers catalyzed by π−Cu(II) complexes†

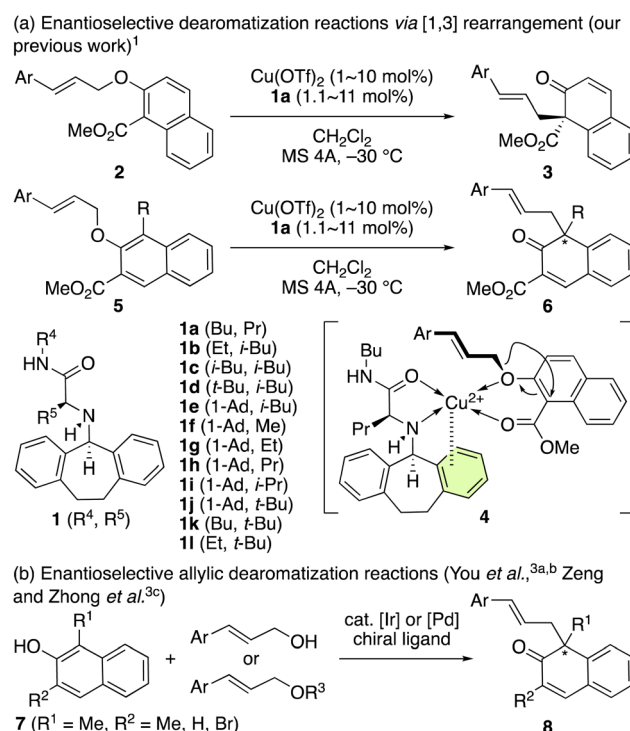Lu Yao,[a] Kazuki Takeda,[a] Kaori Ando [ID] *[b] and Kazuaki Ishihara [ID] *[a]

The first catalytic enantioselective aromatic Claisen rearrangement of allyl 2-naphthyl ethers using 5–10 mol% of π−copper(II) complexes is reported. A Cu(OTf)$_2$ complex with an L-α-homoalanine amide ligand gave (S)-products in up to 92% ee. Conversely, a Cu(OSO$_2$C$_4$F$_9$)$_2$ complex with an L-*tert*-leucine amide ligand gave (R)-products in up to 76% ee. Density-functional-theory (DFT) calculations suggest that these Claisen rearrangements proceed stepwise *via* tight-ion-pair intermediates, and that (S)- and (R)-products are enantioselectively obtained *via* the staggered transition states for the cleavage of the C−O bond, which is the rate-determining step.

Introduction

We have previously developed a chiral π−Cu(II) complex formed from Cu(OTf)$_2$ and chiral ligand **1a** that catalyzes the enantioselective [1,3] O-to-C rearrangement of various methyl 2-(cinnamyloxy)-1-naphthoates (**2**) and methyl 3-(cinnamyloxy)-4-substituted-2-naphthoates (**5**) (Scheme 1a).[1,2] Optically active dearomatized products **3** and **6** can be produced in high enantioselectivity (Scheme 1a), which is induced by the π−Cu(II) interaction in the active intermediate **4**. Independently, alternative methods have been developed by You *et al.*[3a,b] as well as Zeng and Zhong *et al.*[3c] based on the catalytic enantioselective allylic dearomatization of 1,3-dialkyl-2-naphthols (**7**) to give optically active dearomatized products (**8**) which are structurally similar to **6** (Scheme 1b).

Although significant progress has been made in this area,[4] there is still room for the development of other asymmetric catalytic rearrangements. Here we report an enantioselective Claisen rearrangement of methyl 3-(cinnamyloxy)-2-naphthoates (**9**; R^3 = Me) catalyzed by a π−Cu(II) complex to give optically active aromatized products (**10**) (Scheme 2). To the best of our knowledge, this is the first example of a catalytic enantioselective Claisen rearrangement[5,6] of allyl naphthyl ethers and it should be noted here that even examples of non-enantioselective Claisen rearrangements of allyl naphthyl ethers remain scarce to date.[7]

Based on our previous report on [1,3] rearrangements,[1] we began by examining the N-5-dibenzosuberyl-L-leucine-derived amides **1b–e** as chiral ligands in combination with Cu(OTf)$_2$ for the enantioselective Claisen rearrangement of **9a** in dichloromethane (Table 1). The enantioselectivity was increased from 29% ee to 60% ee by using derivatives of **1** with

[a]*Graduate School of Engineering, Nagoya University, B2-3(611) Furo-cho, Chikusa, Nagoya 464-8603, Japan. E-mail: ishihara@cc.nagoya-u.ac.jp*

[b]*Department of Chemistry and Biomolecular Science, Faculty of Engineering, Gifu University, Gifu 501-1193, Japan. E-mail: ando@gifu-u.ac.jp*

† Electronic supplementary information (ESI) available. CCDC 20190517. For ESI and crystallographic data in CIF or other electronic format see DOI: https://doi.org/10.1039/d2sc06771d

Scheme 1 (a) Enantioselective dearomatization of 2-naphthol derivatives *via* [1,3] rearrangement, and (b) dehydrative coupling.

This work
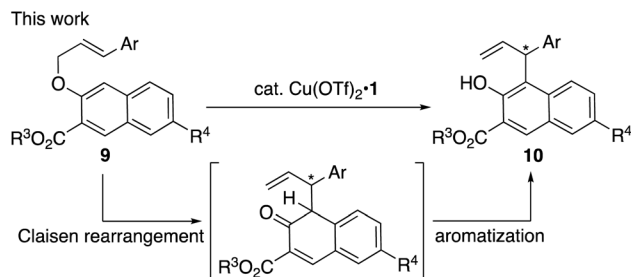
Scheme 2 Catalytic enantioselective aromatic Claisen rearrangement of methyl 3-(cinnamyloxy)-2-naphthoates (**9**, R^3 = Me).

Table 1 Steric effect of the R^4 group of the L-leucine-derived amides (**1b–e**) on the enantioselective aromatic Claisen rearrangement of **9a**[a]

Entry	Ligand **1** (R^4, R^5)	Temp. [°C], time [h]	Product **10a** Conv. [%]	Ee[b] [%]
1	**1b** (Et, i-Bu)	rt,[c] 0.42	>99	29
2	**1c** (i-Bu, i-Bu)	rt,[c] 0.67	>99	30
3	**1d** (t-Bu, i-Bu)	rt,[c] 0.75	>99	42
4	**1e** (1-Ad, i-Bu)[d]	rt,[c] 1	>99	45
5	**1e** (1-Ad, i-Bu)[d]	−20, 5	>99	60
6[e]	**1e** (1-Ad, i-Bu)[d]	−20, 24	>99	70
7	**1e** (1-Ad, i-Bu)[d]	−60, 48	95	66

[a] MS 4A means the zeolite A type, known as LTA (Linde Type A), with 4 Å pore diameter. [b] The absolute configuration was determined in analogy to that of **10f** (Fig. 1). [c] rt = room temperature. [d] 1-Ad = 1-adamantyl. [e] CHCl₃ stabilized with 0.3–1.0% ethanol was used instead of CH₂Cl₂.

Table 2 Steric effect of R^5 of N-(1-adamantyl)amide **1** on the enantioselective aromatic Claisen rearrangement of **9a**[a]

Entry	Ligand **1** (R^4, R^5)	Temp. [°C], time [h]	Product **10a** Conv. [%]	Ee[b] [%]
1	**1f** (1-Ad, Me)	−20, 24	>99	59 (S)
2	**1g** (1-Ad, Et)	−20, 24	>99	73 (S)
3	**1h** (1-Ad, Pr)	−20, 24	>99	73 (S)
4	**1e** (1-Ad, i-Bu)	−20, 24	>99	70 (S)
5	**1i** (1-Ad, i-Pr)	−20, 24	>99	64 (S)
6	**1j** (1-Ad, t-Bu)	rt,[c] 1	>99	28 (R)

[a] CHCl₃ stabilized with 0.3–1.0% ethanol was used as the solvent. MS 4A means the zeolite A type, known as LTA (Linde Type A), with 4 Å pore diameter. [b] The absolute configuration was determined in analogy to that of **10f** (Fig. 1). [c] rt = room temperature.

effective for increasing the enantioselectivity without any significant suppression of the reactivity (entries 3 and 5). When Cu(OSO₂C₄F₉)₂ was used instead of Cu(OTf)₂, the enantioselectivity did not increase (entry 3 vs. entry 4). Thus, the desired product (**10a**) was obtained in 96% conversion with 81% ee under the optimal conditions (entry 6).
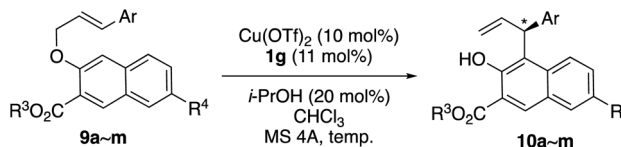
The substrate scope of the enantioselective aromatic Claisen rearrangement of **9a–m** catalyzed by Cu(OTf)₂·**1g** in chloroform is shown in Table 4. Methyl ester **9a** was obtained in a higher enantioselectivity than ethyl ester **9b** (entry 1 vs. entry 2). Higher enantioselectivity was observed in the rearrangement of those substrates bearing electron-withdrawing groups (**9c–i**) (entries 3–10). In contrast, a substrate bearing an electron-donating

Table 3 Additive effect on the enantioselective aromatic Claisen rearrangement of **9a**[a]

Entry	Additive [mol%]	Temp. [°C], time [h]	Product **10a** Conv. [%]	Ee[b] [%]
1	—	−10, 1	>99	60
2[c]	—	−10, 24	>99	72
3	i-PrOH (20)	−10, 1.5	>99	73
4[d]	i-PrOH (20)	−10, 24	>99	70
5	t-BuOH (20)	−10, 1	>99	73
6	i-PrOH (20)	−35, 24	96	81
7	i-PrOH (20)	−40, 24	62	82

[a] Unless otherwise noted, CHCl₃ stabilized with 0.015% 2-methyl-2-butene was used as the solvent. MS 4A means the zeolite A type, known as LTA (Linde Type A), with 4 Å pore diameter. [b] The absolute configuration was determined in analogy to that of **10f** (Fig. 1). [c] CHCl₃ stabilized with 0.3–1.0% ethanol was used as the solvent. [d] Cu(OSO₂C₄F₉)₂ was used instead of Cu(OTf)₂.

more sterically bulky R^4 groups (entries 1–4) at lower temperature (entries 5–7). Interestingly, the enantioselectivity was further increased to 70% ee by using chloroform as the solvent instead of dichloromethane (entry 5 vs. entry 6).

Next, N-5-dibenzosuberyl-L-amino acid-derived N-(1-adamantyl)amides **1e–j** were examined as chiral ligands in combination with Cu(OTf)₂ for the enantioselective Claisen rearrangement of **9a** in chloroform at −20 °C (Table 2). With respect to the enantioselectivity, common primary alkyl groups such as Et and Pr were found to be more suitable R^5 groups than Me, i-Bu and i-Pr (entries 1–5). Interestingly, the absolute stereochemistry of **9a** was reversed for R^5 = t-Bu (entry 6).

In Tables 1 and 2, the experiments in chloroform were carried out using chloroform stabilized with 0.3–1.0% ethanol. To investigate the effect of ethanol on the Claisen rearrangement of **9a**, chloroform stabilized with 0.015% 2-methyl-2-butene was used as a solvent. As shown in Table 3, the enantioselectivity decreased from 72% ee (entry 2) to 60% ee (entry 1) in the absence of ethanol, albeit that the reactivity increased. The addition of 20 mol% of i-PrOH and t-BuOH was also

Table 4 Substrate scope of the enantioselective aromatic Claisen rearrangement of **9** catalyzed by Cu(OTf)$_2$·**1g**[a]
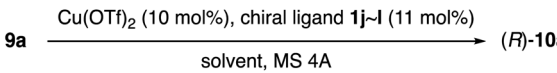
Entry	Substrate **9** (Ar, R^3, R^4)	Temp. [°C], time [h]	Product **10** Yield[b] [%]	Ee[c] [%]
1	**9a** (Ph, Me, H)	−35, 24	92	81 (S)
2	**9b** (Ph, Et, H)	−35, 48	80	77 (S)
3	**9c** (2-ClC$_6$H$_4$, Me, H)	−20, 48	80	82 (R)
4	**9d** (3-ClC$_6$H$_4$, Me, H)	−20, 48	76	84 (S)
5	**9e** (3,5-(CF$_3$)$_2$C$_6$H$_3$, Me, H)	−10, 48	77	89 (S)
6[d]	**9e** (3,5-(CF$_3$)$_2$C$_6$H$_3$, Me, H)	−20, 48	95	92 (S)
7	**9f** (3,5-Br$_2$C$_6$H$_3$, Me, H)	−20, 48	44	84 (S)
8	**9g** (4-ClC$_6$H$_4$, Me, H)	−20, 24	95	81 (S)
9	**9h** (4-BrC$_6$H$_4$, Me, H)	−20, 24	85	82 (S)
10	**9i** (4-CF$_3$C$_6$H$_4$, Me, H)	−20, 48	67	87 (S)
11	**9j** (4-MeC$_6$H$_4$, Me, H)	−20, 24	90	65 (S)
12	**9k** (3-thienyl, Me, H)	−20, 24	80	73 (R)
13	**9l** (Ph, Me, Br)	−20, 24	70	77 (S)
14	**9m** (4-ClC$_6$H$_4$, Me, OMe)	−20, 12	95	85 (S)

[a] Unless otherwise noted, CHCl$_3$ stabilized with 0.015% 2-methyl-2-butene was used as the solvent. MS 4A means the zeolite A type, known as LTA (Linde Type A), with 4 Å pore diameter. [b] Isolated yield. [c] The absolute configuration was determined in analogy to that of **10f** (Fig. 1). [d] Cu(OTf)$_2$ (20 mol%) and **1g** (22 mol%) were used without i-PrOH.

group (**9j**) was more reactive but furnished **10j** in a lower ee (entry 11). 3-(3-Thienyl)allyl naphthyl ether **9k** could also be used as a substrate (entry 12). Interestingly, the 7-bromo group of **9l** decreased both the reactivity and enantioselectivity (entry 1 vs. entry 13), whereas the 7-methoxy group of **9m** increased both the reactivity and enantioselectivity (entry 8 vs. entry 14).

Using single-crystal X-ray diffraction analysis, the absolute configuration of **10f** (entry 7, Table 4) was determined to be (S) (Fig. 1). Thus, the absolute configuration of the other products **10** obtained in Tables 1–4 was determined in analogy to that of **10f**.

This catalytic Claisen rearrangement is scalable. On the gram scale, the rearrangement of **9a** was complete within 7 h in the presence of 5 mol% of Cu(OTf)$_2$·**1g** at −20 °C to give (S)-**10a** in 95% isolated yield with 77% ee (eqn (1)).
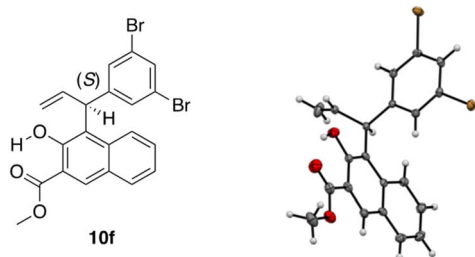
Fig. 1 X-ray structure of product **10f**.

Table 5 Steric effect of R^4 of L-tert-leucine-derived amide **1** on the enantioselective aromatic Claisen rearrangement of **9a**[a]

Entry	Ligand **1** (R^4)	Solvent, temp. [°C], time [h]	Product **10a** Conv. [%]	Ee[b] [%]
1	**1j** (1-Ad)[c]	CH$_2$Cl$_2$, rt,[d] 1	>99	28
2	**1k** (Bu)	CH$_2$Cl$_2$, rt,[d] 0.5	>99	45
3	**1l** (Et)	CH$_2$Cl$_2$, rt,[d] 0.5	>99	43
4[e]	**1k** (Bu)	CHCl$_3$, −10, 6	>99	61
5[e]	**1k** (Bu)	CHCl$_3$, −30, 48	97	68
6[e,f]	**1k** (Bu)	CHCl$_3$, −30, 48	33	68
7[e,g]	**1k** (Bu)	CHCl$_3$, −30, 48	95	71

[a] MS 4A means the zeolite A type, known as LTA (Linde Type A), with 4 Å pore diameter. [b] The absolute configuration was determined in analogy to that of **10f** (Fig. 1). [c] 1-Ad = 1-adamantyl. [d] rt = room temperature. [e] CHCl$_3$ stabilized with 0.015% 2-methyl-2-butene was used. [f] 20 mol% of i-PrOH was added. [g] Cu(OSO$_2$C$_4$F$_9$)$_2$ was used instead of Cu(OTf)$_2$.

(1)
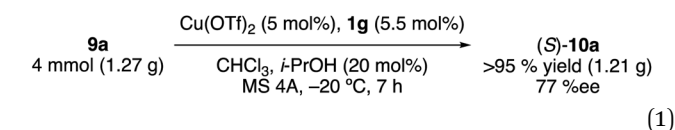
Next, we focused on the inverse asymmetric induction observed in entry 6 of Table 2. To improve the enantioselectivity, the R^4 group of ligand **1** was optimized to improve the enantioselectivity (Table 5). Primary alkyl groups such as Et and Bu were found to be more suitable than bulkier groups such as Ad (entries 1–3). In terms of the enantioselectivity, chloroform was better than dichloromethane (entry 2 vs. entry 4). The addition of i-PrOH decreased the catalytic activity and did not influence the enantioselectivity (entry 5 vs. entry 6). An enantioselectivity of 67% ee was observed when using Cu(OTf)$_2$·**1k** in chloroform at −30 °C (entry 6). The enantioselectivity increased to 71% ee when Cu(OSO$_2$C$_4$F$_9$)$_2$ was used instead of Cu(OTf)$_2$ (entry 7).

As shown in Table 6, substrates **9g**, **9j**, and **9a**, were also transformed to **10** with moderate enantioselectivity in the presence of Cu(OSO$_2$C$_4$F$_9$)$_2$·**1k**.

Finally, we turned our attention to the mechanism of the reaction. For that purpose, a crossover experiment using a mixture of substrates **9g** and **9b** in the presence of 10 mol% of Cu(OTf)$_2$·**1g** in chloroform was conducted (Scheme 3). The intramolecular rearrangements of **9g** and **9b** proceeded smoothly and no crossover products were obtained. Therefore, it was ascertained that this reaction proceeds via a concerted or tight-ion-pair pathway.

To understand the origin of the enantioselectivity of this reaction, we performed density-functional-theory (DFT) calculations at the B3LYP/6-31G(d) and LANL2DZ for Cu(II) level (Gaussian 16 (ref. 8)). At first, we studied the complexation of substrate **9a** with catalyst Cu(OTf)$_2$·**1**. There are two possible

Table 6 The enantioselective aromatic Claisen rearrangement of **9** catalyzed by Cu(OSO₂C₄F₉)₂·**1k**[a]
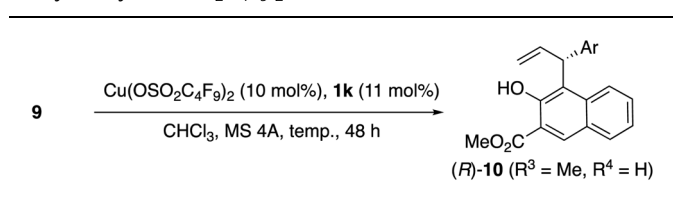
Entry	Substrate **9** (Ar, R³, R⁴)	Temp. [°C]	Product **10**	
			Yield[b] [%]	Ee[c] [%]
1	**9a** (Ph, Me, H)	−30	95	71 (R)
2	**9g** (4-Cl-C₆H₄, Me, H)	−20	64	76 (R)
3	**9j** (4-MeC₆H₄, Me, H)	−30	88	72 (R)

[a] CHCl₃ stabilized with 0.015% 2-methyl-2-butene was used. MS 4A means the zeolite A type, known as LTA (Linde Type A), with 4 Å pore diameter. [b] Isolated yield. [c] The absolute configuration was determined by analogy with that of **10f** (Fig. 1).
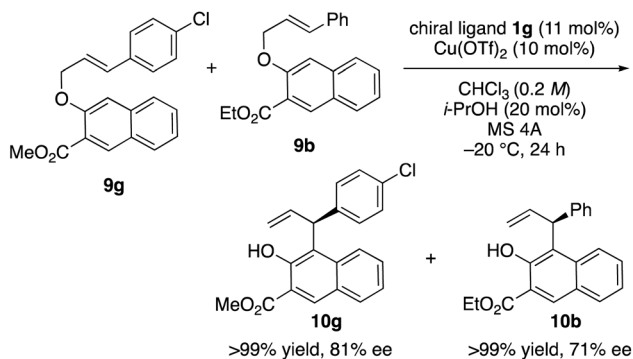
Scheme 3 Crossover experiment.

geometrical chelate structures for the complex between **9a** and Cu(OTf)₂·**1**. In the case of Cu(OTf)₂·**1g**, one triflate anion is released from Cu(II) by chelation of **9a** (Fig. 2). The *trans* structure of **9a**·Cu(OTf)⁺·**1g**, wherein the ether oxygen is located *trans* to the nitrogen of **1g**, is 9.3 kcal mol⁻¹ more stable than the *cis* structure, which is unstable due to steric hindrance between the axial hydrogen of *N*-5-dibenzosuberyl of **1g** and one of the OCH₂ hydrogens of **9a**.[9] Here, the H–H distance (2.28 Å) is shorter than the sum of their van der Waals radii (2.40 Å).
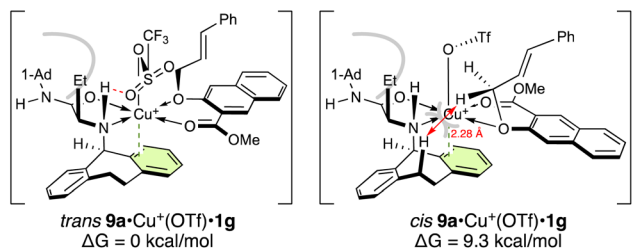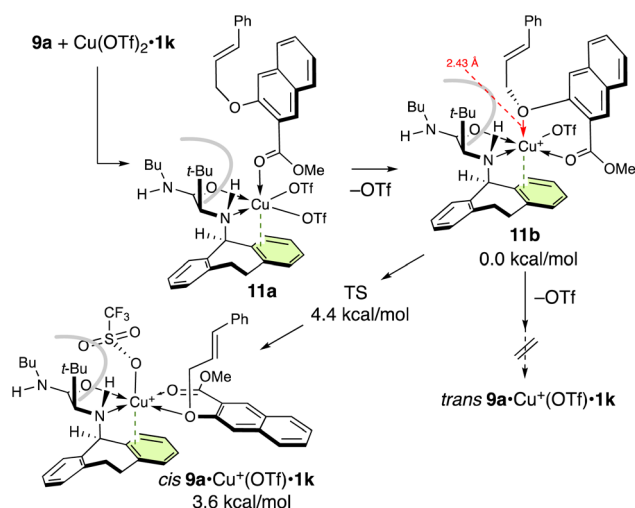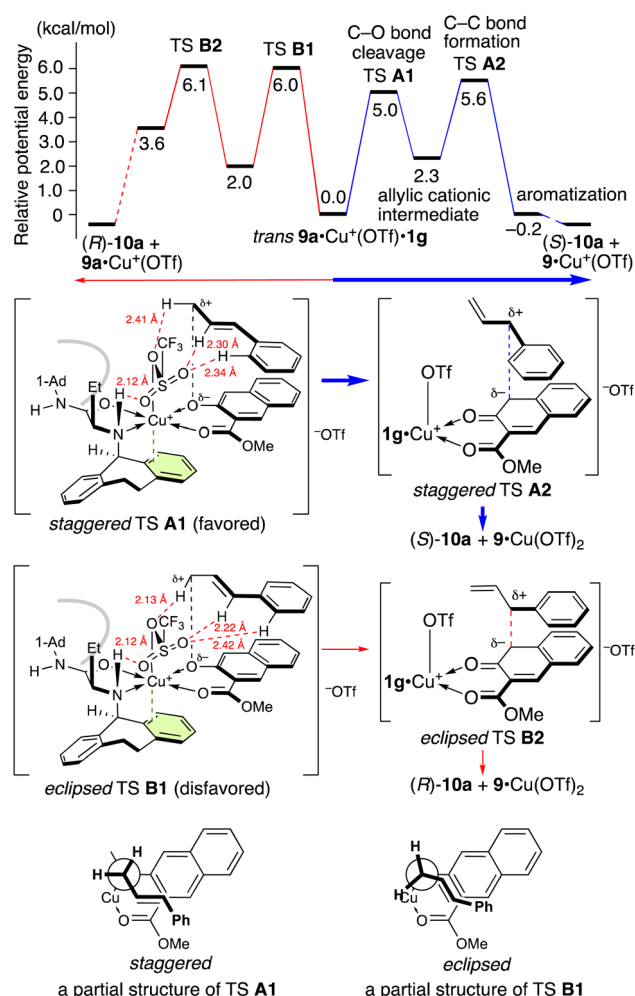

Fig. 2 Two geometrical structures of **9a**·Cu(OTf)⁺·**1g**. For computational details, see the ESI.†

Scheme 4 Potential energy profile at 25 °C and the complexation of **9a** with Cu(OTf)₂·**1k**.[a] [a]For computational details, see the ESI.†

Scheme 5 Potential energy profile at 25 °C and transition states for the aromatic Claisen rearrangement of **9a** catalyzed by Cu(OTf)₂·**1g**.[a] [a]For computational details, see the ESI.†

Next, we studied the complexation of **9a** with Cu(OTf)$_2$·**1k** (Scheme 4). Interestingly, *cis* **9a**·Cu$^+$(OTf)·**1k** is predominantly formed *via* monocoordinated complex **11a**. On the other hand, *trans* **9a**·Cu$^+$(OTf)·**1k** is not obtained from **11a** due to the steric demand of the *t*-butyl group. When the ether oxygen of **11a** is moved closer to Cu(II), one of the triflates is easily eliminated to give **11b**. Subsequently, the ether oxygen of **11b** approaches Cu(II) and the triflate is repelled to the apical position to form *cis* **9a**·Cu$^+$(OTf)·**1k** (for details, see the ESI†).

Interestingly, the Claisen rearrangement of **9a** proceeds stepwise *via* a tight-ion-pair intermediate. Both potential energy profiles that lead to enantiomeric products (*S*)-**10a** and (*R*)-**10a** are shown in Schemes 5 and 6. Substrate **9a** predominantly chelates to Cu(OTf)$_2$·**1g** in a *trans* manner between the nitrogen atom of **1g** and the ether oxygen atom of **9a** due to steric and electronic effects (for details, see the ESI†). One triflate anion is released from Cu(II) due to the π–Cu(II) interaction to generate [**9a**·Cu$^+$(OTf)·**1g**][$^-$OTf]. Another triflate group occupies the apical position of the octahedral Cu(II) complex, avoiding the bulky *N*-1-adamantyl group of **1g**. Both the transition structures **A1** and **B1** for the cleavage of the C–O bond are stabilized by hydrogen bonding between the allylic protons and the triflate oxygens. Staggered transition state (TS) **A1** is more stable than eclipsed TS **B1** due to torsional effect (mainly electronic repulsion). Thus, (*S*)-**10a** is obtained as the major enantiomer *via* TS **A1**. Although the energy values of TSs **A2** and **B2** for the formation of the C–C bond are slightly higher than those of **A1** and **B1**, the lack of crossover products suggests that cleavage of the C–O bond is the rate-limiting step. This energy difference between TSs **A1** and **B1** is 0.97 kcal mol^{-1} at 25 °C and 1.17 kcal mol^{-1} at −35 °C, corresponding to 84% ee at −35 °C. This energy difference is in good agreement with the experimental results (entry 1 in Table 4).

In contrast, when **1k** is used, *cis* **9a**·Cu$^+$(OTf)·**1k** is preferred (Scheme 4). The apical triflate group is positioned to avoid steric hindrance of the *t*-butyl group and cannot be stabilized by a hydrogen bonding with the amino protons (TS **C1** and TS **D1** in Scheme 6). The staggered TS **D1** is favored compared to the eclipsed TS **C1** due to the torsional effect. Thus, (*R*)-**10a** is obtained as a major enantiomer *via* TS **D1**. The energy difference between TSs **D1** and **C1** is 0.72 kcal mol^{-1} at 25 °C and 0.80 kcal mol^{-1} at −30 °C, corresponding to 68% ee at −30 °C. This energy difference is in good agreement with the experimental results (entry 5 in Table 5).

Scheme 6 Potential energy profile at 25 °C and the transition states for the aromatic Claisen rearrangement of **9a** catalyzed by Cu(OTf)$_2$-·**1k**.^{a} ^{a}For computational details, see the ESI.†

Conclusions

In summary, we have accomplished the first catalytic enantioselective aromatic Claisen rearrangement of allyl 2-naphthyl ethers **9** by using a chiral π–Cu(II) catalyst. The Cu(OTf)$_2$ complex with L-α-homoalanine amide ligand **1g** gave (*S*)-**10** products in up to 92% ee. Conversely, the Cu(OSO$_2$C$_4$F$_9$)$_2$ complex with L-*tert*-leucine amide ligand **1k** gave (*R*)-**10** products in up to 71% ee. DFT calculations suggest that the preference of these catalysts for (*S*)- and (*R*)-products might be ascribed to a preference of the reactions to proceed *via* a staggered rather than an eclipsed transition state.
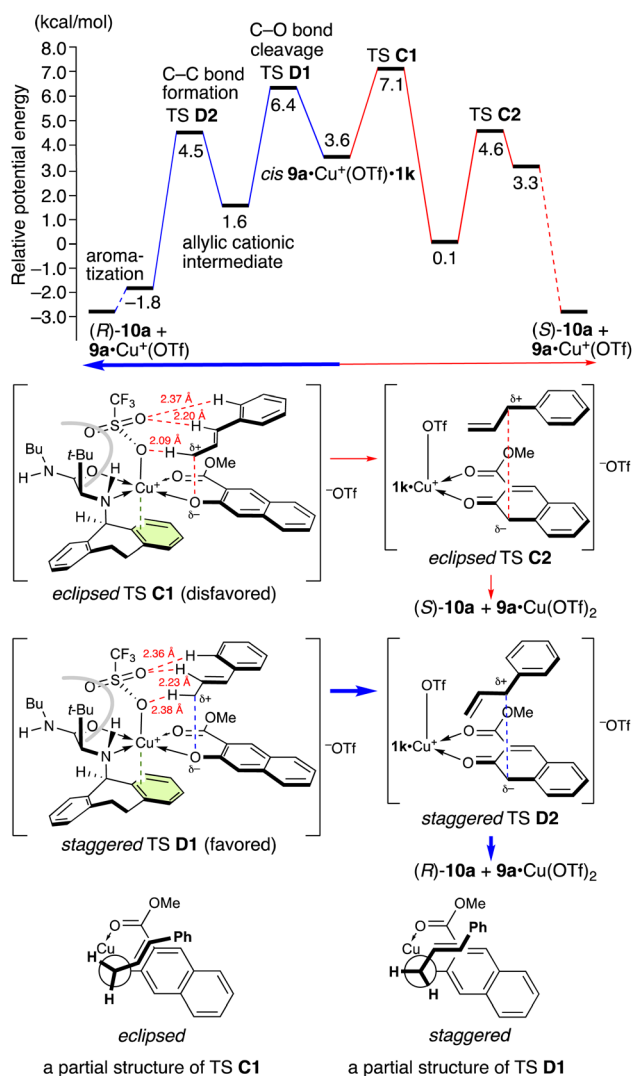
Data availability

All experimental procedures, spectral data and computational calculations are available in the ESI.†

Author contributions

K. I. conceived and directed the project. L. Y. and K. T. carried out the experiments and collected data. K. A. performed and analyzed the DFT calculations. K. I. wrote the manuscript with contributions from all authors.

Conflicts of interest

There are no conflicts to declare.

Acknowledgements

Notes and references

1 L. Yao and K. Ishihara, *Chem. Sci.*, 2019, **10**, 2259–2263.

2 (*a*) K. Ishihara and M. Fushimi, *Org. Lett.*, 2006, **8**, 1921–1924; (*b*) K. Ishihara, M. Fushimi and M. Akakura, *Acc. Chem. Res.*, 2007, **40**, 1049–1055; (*c*) K. Ishihara and M. Fushimi, *J. Am. Chem. Soc.*, 2008, **130**, 7532–7533; (*d*) A. Sakakura, M. Hori, M. Fushimi and K. Ishihara, *J. Am. Chem. Soc.*, 2010, **132**, 15550–15552; (*e*) A. Sakakura and K. Ishihara, *Chem. Soc. Rev.*, 2011, **40**, 163–172; (*f*) M. Hori, A. Sakakura and K. Ishihara, *J. Am. Chem. Soc.*, 2014, **136**, 13198–13201; (*g*) K. Ishihara, K. Nishimura and K. Yamakawa, *Angew. Chem., Int. Ed.*, 2020, **59**, 17641–17647; (*h*) K. Nishimura, Y. Wang, Y. Ogura, J. Kumagai and K. Ishihara, *ACS Catal.*, 2022, **12**, 1012–1017; (*i*) K. Nishimura and K. Ishihara, *Synlett*, 2022, **33**, 585–588; (*j*) K. Nishimura, Y. Ogura, K. Takeda, W. Guo and K. Ishihara, *Org. Lett.*, 2022, **24**, 7685–7689.

3 (*a*) C.-X. Zhuo and S.-L. You, *Angew. Chem., Int. Ed.*, 2013, **52**, 10056–10059; (*b*) H.-F. Tu, C. Zheng, R.-Q. Xu, X.-J. Liu and S.-L. You, *Angew. Chem., Int. Ed.*, 2017, **56**, 3237–3241; (*c*) D. Shen, Q. Chen, P. Yan, X. Zeng and G. Zhong, *Angew. Chem., Int. Ed.*, 2017, **56**, 3242–3246.

4 (*a*) L. Wang, P. Zhou, Q. Lin, S. Dong, X. Liu and X. Feng, *Chem. Sci.*, 2020, **11**, 10101–10106; (*b*) H. Zheng, Y. Wang, C. Xu, X. Xu, L. Lin, X. Liu and X. Feng, *Nat. Commun.*, 2018, **9**, 1968.

5 Taguchi *et al.* have reported an enantioselective aromatic Claisen rearrangement using 150 mol% of chiral Lewis acid; for details see: H. Ito, A. Sato and T. Taguchi, *Tetrahedron Lett.*, 1997, **38**, 4815–4818.

6 For the examples of asymmetric Claisen rearrangements of propargyl ethers, see: (*a*) Y. Liu, H. Hu, H. Zheng, Y. Xia, X. Liu, L. Lin and X. Feng, *Angew. Chem., Int. Ed.*, 2014, **53**, 11579–11582; (*b*) L. Wang, Y. Zhou, Z. Su, F. Zhang, W. Cao, X. Liu and X. Feng, *Angew. Chem., Int. Ed.*, 2022, **61**, e202211785.

7 T. Ollevier and T. M. Mwene-Mbeja, *Tetrahedron Lett.*, 2006, **47**, 4051–4055.

8 M. J. Frisch, G. W. Trucks, H. B. Schlegel, G. E. Scuseria, M. A. Robb, J. R. Cheeseman, G. Scalmani, V. Barone, G. A. Petersson, H. Nakatsuji, X. Li, M. Caricato, A. V. Marenich, J. Bloino, B. G. Janesko, R. Gomperts, B. Mennucci, H. P. Hratchian, J. V. Ortiz, A. F. Izmaylov, J. L. Sonnenberg, D. Williams-Young, F. Ding, F. Lipparini, F. Egidi, J. Goings, B. Peng, A. Petrone, T. Henderson, D. Ranasinghe, V. G. Zakrzewski, J. Gao, N. Rega, G. Zheng, W. Liang, M. Hada, M. Ehara, K. Toyota, R. Fukuda, J. Hasegawa, M. Ishida, T. Nakajima, Y. Honda, O. Kitao, H. Nakai, T. Vreven, K. Throssell, J. A. Montgomery Jr, J. E. Peralta, F. Ogliaro, M. J. Bearpark, J. J. Heyd, E. N. Brothers, K. N. Kudin, V. N. Staroverov, T. A. Keith, R. Kobayashi, J. Normand, K. Raghavachari, A. P. Rendell, J. C. Burant, S. S. Iyengar, J. Tomasi, M. Cossi, J. M. Millam, M. Klene, C. Adamo, R. Cammi, J. W. Ochterski, R. L. Martin, K. Morokuma, O. Farkas, J. B. Foresman and D. J. Fox, *Gaussian 16, Revision C.01*, Gaussian, Inc., Wallingford CT, 2019.

9 The energy difference of 9.3 kcal mol^{-1} is very large. To clarify this result, we performed optimization and energy calculations of complexes *trans*-**9a**·Cu^{+}(OTf)·**1**′ and *cis*-**9a**·Cu^{+}(OTf)·**1**′ using sterically less hindered *N*-methylglycine *N*-methylamide (**1**′) instead of **1g**. *trans*-**9a**·Cu^{+}(OTf)·**1**′, wherein the ether oxygen located *trans* to the amino nitrogen, is 5.5 kcal mol^{-1} more stable than *cis*-**9a**·Cu^{+}(OTf)·**1**′. Given that no steric hindrance is observed in *cis*-**9a**·Cu^{+}(OTf)·**1**′, the instability of *cis*-**9a**·Cu^{+}(OTf)·**1**′ was attributed to the electronic effect of nitrogen.